

# Prenatal Stress Detection from Electrocardiography Using Self-Supervised Deep Learning: Development and External Validation

Martin G. Frasch<sup>1,2,\*</sup>, Marlene J.E. Mayer<sup>3</sup>, Clara Becker<sup>3</sup>, Peter  
Zimmermann<sup>3</sup>, Camilla Zelgert<sup>3</sup>, Marta C. Antonelli<sup>4,5</sup>, and Silvia M.  
Lobmaier<sup>3</sup>

<sup>1</sup>*Institute on Human Development and Disability, University of Washington,  
Seattle, WA, USA*

<sup>2</sup>*JoyBeat Medical, Seattle, WA, USA*

<sup>3</sup>*Department of Obstetrics and Gynecology, TUM University Hospital,  
Technical University of Munich, Munich, Germany*

<sup>4</sup>*Technical University of Munich; Institute for Advanced Study, Garching,  
Germany*

<sup>5</sup>*Instituto de Biología Celular y Neurociencia “Prof. Eduardo De Robertis”,  
Facultad de Medicina, Universidad de Buenos Aires, Argentina*

\* *Corresponding author: mfrasch@uw.edu*

## Abstract

**Background:** Prenatal psychological stress affects 15–25% of pregnancies and increases risks of preterm birth, low birth weight, and adverse neurodevelopmental outcomes. Current screening relies on subjective questionnaires (PSS-10), limiting continuous monitoring and objective assessment.

**Methods:** We developed deep learning models for automated stress detection from electrocardiography (ECG) using the FELICITY 1 cohort (151 pregnant women, 32–38 weeks gestation, Monica AN-24 device, 900 Hz sampling). A ResNet-34 encoder (16.7M parameters) was pretrained via SimCLR contrastive learning on 40,692 ECG segments per subject. Multi-layer feature extraction (1088 dimensions) enabled both binary classification (stressed vs. non-stressed) and continuous PSS prediction. We tested maternal ECG (mECG), fetal ECG (fECG), and abdominal ECG (aECG). External validation was performed on the FELICITY 2 randomized controlled trial (28 subjects, Bittium Faros 360 device, 1000 Hz sampling, yoga intervention vs. control).

**Results:** Using subject-stratified 5-fold cross-validation on FELICITY 1, the ResNet multi-layer approach achieved: mECG 98.6% accuracy ( $R^2=0.88$ , MAE=1.90 PSS points), fECG 99.8% accuracy ( $R^2=0.95$ , MAE=1.19), and aECG 95.5% accuracy ( $R^2=0.75$ , MAE=2.80). External validation on FELICITY 2 demonstrated strong generalization: mECG achieved 77.3% accuracy ( $R^2=0.62$ , MAE=3.54 PSS points, AUC=0.826) and aECG achieved 63.6% accuracy ( $R^2=0.29$ , MAE=4.18, AUC=0.705). Signal quality-based channel selection outperformed all-channel averaging (+12%  $R^2$  improvement). Mixed-effects models detected significant intervention response (visit $\times$ group interaction  $p=0.041$ ).

**Conclusions:** Self-supervised deep learning on pregnancy ECG enables highly accurate, objective stress assessment. Multi-layer feature extraction substantially outperforms single embedding approaches. This technology could enable continuous prenatal stress monitoring and early intervention targeting.

**Keywords:** prenatal stress, electrocardiography, deep learning, self-supervised learning, SimCLR, pregnancy monitoring

# 1 Introduction

Prenatal psychological stress affects 15–25% of pregnancies and represents a major public health concern with substantial maternal and fetal consequences[1, 2, 3]. Elevated maternal stress during pregnancy is associated with increased risks of preterm birth, low birth weight, pre-eclampsia, and adverse long-term neurodevelopmental outcomes in offspring[4, 5, 6]. Despite well-established consequences, prenatal stress screening in clinical practice relies predominantly on subjective self-report questionnaires, most commonly the Perceived Stress Scale (PSS-10)[7]. While PSS-10 provides validated stress assessment, its subjective nature, snapshot-based administration, and reliance on patient recall limit its utility for continuous monitoring, early detection, and real-time intervention.

Physiological measurement of stress offers complementary objective assessment. The autonomic nervous system responds to psychological stress through measurable changes in heart rate variability (HRV), cardiac rhythm patterns, and electrodermal activity[8, 9]. During pregnancy, these autonomic markers can be captured non-invasively through electrocardiography (ECG), providing continuous, objective stress-related signals from both the mother and developing fetus[10, 11, 12]. Previous studies have demonstrated associations between prenatal stress and altered maternal HRV[13, 14], as well as stress-related changes in fetal heart rate patterns[15, 16]. However, translation of these findings into clinically deployable automated screening systems has been limited by small sample sizes, reliance on hand-crafted features, and insufficient external validation.

Recent advances in deep learning and self-supervised representation learning offer new opportunities for automated physiological signal analysis. Convolutional neural networks (CNNs), particularly residual architectures (ResNets), have demonstrated exceptional performance in ECG analysis tasks including arrhythmia detection, myocardial infarction diagnosis, and cardiovascular risk prediction[17, 18, 19]. Self-supervised learning methods such as SimCLR (Simple Framework for Contrastive Learning of Visual Representations)[20] enable models to learn robust representations from unlabeled data through contrastive objectives, reducing dependence on extensive manual annotation. Furthermore, recent foundation models pretrained on large-scale ECG databases[21, 22] offer transferable representations that may enhance performance on downstream clinical tasks.

Despite these technical advances, critical gaps remain in applying deep learning to prenatal stress detection. First, most ECG-based stress detection studies have focused on non-pregnant populations or used shallow machine learning with hand-crafted features[23, 24]. Second, the relative utility of different ECG sources during pregnancy (maternal chest ECG, fetal ECG extracted from abdominal recordings, or raw abdominal ECG) for stress detection remains unclear. Third, the optimal feature extraction strategy—whether to use final layer embeddings from pretrained models, intermediate layer features, or combinations of multiple representation levels—has not been systematically evaluated for stress detection. Finally, and most critically, external validation on independent cohorts is rarely performed, limiting assessment of model generalizability.

In this study, we address these gaps through development and rigorous validation of deep learning models for automated prenatal stress detection from ECG. We leveraged the FELICITY 1 cohort (151 pregnant women with concurrent PSS-10 and multi-modal ECG recordings) to train and internally validate models, followed by external validation on the FE-

LICITy 2 randomized controlled trial of yoga intervention for stress reduction. We compared multiple representation learning strategies including: (1) ResNet-34 with SimCLR pretraining, (2) multi-layer feature extraction from all ResNet intermediate layers, and (3) integration with ECGFounder foundation model embeddings. We hypothesized that multi-layer feature extraction would capture complementary stress-related patterns across representation hierarchies, improving performance beyond single-layer approaches. We further hypothesized that models trained on FELICITy 1 would generalize to FELICITy 2, enabling detection of both stress levels and intervention-induced stress reduction.

## 2 Methods

### 2.1 Study Design and Participants

This study analyzed data from two independent pregnancy cohorts: FELICITy 1 for model development and internal validation, and FELICITy 2 for external validation.

#### 2.1.1 FELICITy 1 Cohort (Development)

The FELICITy 1 study enrolled 151 pregnant women at 32–38 weeks gestation between June 2016 and July 2019. Inclusion criteria required singleton pregnancy with planned delivery at the study hospital. Exclusion criteria included known major fetal anomalies, maternal cardiac arrhythmias, or maternal medications affecting autonomic function. All participants provided written informed consent under IRB protocol approved by the Committee of Ethical Principles for Medical Research at the TUM (registration number 151/16S; ClinicalTrials.gov registration number NCT03389178).

At enrollment, participants completed the Perceived Stress Scale (PSS-10), a validated 10-item questionnaire assessing perceived stress over the preceding month[7]. PSS-10 scores range from 0–40, with scores  $\geq 14$  indicating moderate-to-high stress[25]. Concurrent with PSS-10 assessment, participants underwent 10-minute ECG recordings in a quiet, temperature-controlled room using a 5-electrode abdominal array (Monica AN-24, Monica Healthcare Ltd, Nottingham, UK) for simultaneous maternal and fetal ECG acquisition (sampling rate 900 Hz).

#### 2.1.2 FELICITy 2 Cohort (External Validation)

The FELICITy 2 study was a randomized controlled trial evaluating prenatal yoga intervention for stress reduction. Participants ( $n=28$ ) were enrolled at  $\sim 32$  weeks gestation with baseline PSS-10  $\geq 19$  (high stress) and randomized 1:1 to yoga intervention (weekly 90-minute sessions for 6 weeks) or standard care control. PSS-10 and 10-minute abdominal ECG recordings were collected using a different device than FELICITy 1: the Bittium Faros 360 (Bittium Corporation, Oulu, Finland), a 3-channel ambulatory ECG recorder with 1000 Hz sampling rate. Recordings were collected at baseline ( $\sim 32$  weeks) and follow-up ( $\sim 38$  weeks). The study was approved under IRB protocol (approval number 2022-86-S-SR, 6 September 2022) with written informed consent. Importantly, the difference in recording

hardware (Monica AN-24 at 900 Hz vs. Bittium Faros 360 at 1000 Hz) between cohorts represents a deliberate test of model robustness to hardware-induced variance.

## 2.2 ECG Acquisition and Preprocessing

Three ECG signal types were extracted and analyzed:

**Maternal ECG (mECG):** Standard 12-lead recordings were processed using lead II. Raw signals were bandpass filtered (0.5–40 Hz) to remove baseline wander and high-frequency noise, then resampled from 1000 Hz to 256 Hz using polyphase anti-aliasing.

**Fetal ECG (fECG):** Extracted from 5-electrode abdominal array recordings using the SAVER (Smart Adaptive Ecg Recognition) algorithm[26]. SAVER performs blind source separation optimized for fetal QRS complex morphology, followed by validation using fetal heart rate constraints (110–180 bpm). Extracted fECG signals underwent identical preprocessing (0.5–40 Hz bandpass, resampling to 256 Hz).

**Abdominal ECG (aECG):** Raw abdominal recordings were preprocessed without fECG extraction, preserving the composite maternal-fetal signal. This represents a clinically practical approach requiring no source separation, suitable for continuous monitoring applications.

All preprocessed signals were segmented into 10-second windows (2560 samples at 256 Hz) with 50% overlap, yielding  $\sim 40,000$  segments per subject per ECG type. Segments with excessive artifact (defined as signal amplitude  $>10\times$  median or flat-line  $>1$  second) were excluded. **Critically, subject-stratified data splitting was performed *before* segmentation to ensure no data leakage:** subjects were first assigned to cross-validation folds, then segmentation was applied within each fold. This prevents overlapping windows from the same recording appearing in both training and test sets. Z-score normalization was applied per-segment using training set statistics only.

## 2.3 Deep Learning Architecture

### 2.3.1 ResNet-34 Encoder with SimCLR Pretraining

We employed a ResNet-34 convolutional neural network[27] adapted for 1D ECG signals as the primary feature encoder (16.7M parameters). The architecture consists of:

- Initial  $7\times 1$  convolutional layer (64 filters, stride=2)
- Max pooling ( $3\times 1$ , stride=2)
- Four residual blocks with [3, 4, 6, 3] layers respectively
- Channel dimensions: [64, 128, 256, 512]

The encoder was pretrained using SimCLR (Simple Framework for Contrastive Learning)[20], a self-supervised contrastive learning method. For each ECG segment, two augmented views were generated through:

1. Gaussian noise injection ( $\sigma=0.1$ )

2. Time shifting ( $\pm 5\%$  of segment length)
3. Amplitude scaling ( $0.9\text{--}1.1\times$ )
4. Time warping ( $0.95\text{--}1.05\times$  speed)

SimCLR training optimized the NT-Xent (normalized temperature-scaled cross entropy) loss to maximize agreement between augmented views of the same segment while minimizing agreement with other segments. A 2-layer MLP projection head ( $512\rightarrow 128$  dimensions) mapped encoder outputs to the contrastive learning space. Training used batch size 256, temperature  $\tau=0.5$ , learning rate  $3\times 10^{-4}$  with cosine annealing, and 100 epochs per ECG type.

### 2.3.2 Multi-Layer Feature Extraction

Rather than using only final-layer embeddings, we extracted and concatenated features from all ResNet intermediate layers plus the projection head:

- **Layer 1 output:** 64 dimensions (low-level morphology)
- **Layer 2 output:** 128 dimensions (intermediate patterns)
- **Layer 3 output:** 256 dimensions (complex motifs)
- **Layer 4 output:** 512 dimensions (high-level representations)
- **Projection head:** 128 dimensions (contrastive space)

Global average pooling was applied to each layer’s spatial dimension, yielding a concatenated 1088-dimensional feature vector. This multi-layer approach captures stress-related patterns across multiple representation levels: early layers preserve signal morphology (QRS complex shape, baseline dynamics), while deeper layers encode higher-order temporal dependencies and complex rhythm patterns.

### 2.3.3 ECGFounder Foundation Model

For comparison, we evaluated ECGFounder[21], a foundation model pretrained on 10 million ECG segments from diverse clinical datasets. ECGFounder employs a Vision Transformer (ViT) architecture with 12 attention layers, generating 512-dimensional embeddings. **ECG-Founder was used purely for feature extraction (inference-only mode) without fine-tuning**, as we sought to evaluate the utility of general-purpose ECG representations for the specific task of stress detection. We extracted ECGFounder embeddings for all FELICITY 1 segments using the official pretrained model weights deployed via a remote API inference service on Google Cloud Run.

## 2.4 Stress Classification and Regression Models

For each feature representation (ResNet multi-layer, ResNet final-layer only, ECGFounder, or combinations), we trained downstream models for two tasks:

**Binary Classification:** Logistic regression with L2 regularization ( $C=1.0$ ) predicted binary stress status ( $PSS-10 \geq 19$ ). Subject-stratified 5-fold cross-validation ensured no subject’s segments appeared in both training and test sets. Performance metrics included accuracy, precision, recall, F1-score, and area under ROC curve (AUC) with 95% confidence intervals.

**PSS Regression:** Ridge regression ( $\alpha=1.0$ ) predicted continuous PSS-10 scores. Performance was assessed via coefficient of determination ( $R^2$ ), mean absolute error (MAE), root mean squared error (RMSE), and Pearson correlation with 95% confidence intervals.

For segment-level predictions, subject-level scores were computed by averaging predictions across all segments for each participant.

## 2.5 Signal Quality Assessment for FELICITY 2

FELICITY 2 recordings contained 3 ECG channels per file. To determine optimal channel selection, we implemented comprehensive signal quality index (SQI) assessment adapted from established methods for fetal ECG quality evaluation[28]. For each channel, four SQI components were computed:

1. **Template Matching SQI** (40% weight): QRS complex morphology consistency measured via Pearson correlation between individual beats and mean template
2. **RR Interval Consistency SQI** (30% weight): Heart rate variability stability quantified through coefficient of variation of RR intervals
3. **Baseline Stability SQI** (20% weight): Low-frequency drift assessment via baseline wander amplitude
4. **Amplitude Consistency SQI** (10% weight): QRS amplitude variance across the recording

Overall SQI was computed as the weighted sum, with values  $>0.5$  indicating acceptable quality.

We tested two inference strategies:

- **Approach A (SQI-Selected):** Select the single highest-SQI channel per recording for prediction
- **Approach B (All-Channel Average):** Compute predictions from all 3 channels independently and average results

## 2.6 Statistical Analysis

**FELICITY 1 Internal Validation:** Subject-stratified 5-fold cross-validation with 5 repetitions (25 total folds) assessed model performance and stability. Confidence intervals (95%) were computed via bootstrap resampling (1000 iterations).

**FELICITY 2 External Validation:** Model performance on unseen FELICITY 2 data tested generalization. Temporal analysis used mixed-effects models with PSS as outcome, fixed effects of visit (baseline/follow-up) and group (yoga/control), and random intercepts for subjects. The visit $\times$ group interaction term tested differential intervention effects. Missing data were handled via maximum likelihood estimation for regression/classification (using all available recordings) and complete-case analysis for paired temporal changes.

Group comparisons used independent  $t$ -tests for continuous measures and chi-square tests for binary outcomes. Effect sizes were quantified via Cohen’s  $d$ . Statistical significance was set at  $p < 0.05$  (two-tailed). Analyses used Python 3.10 with scikit-learn 1.3, statsmodels 0.14, and scipy 1.11.

## 2.7 Code and Data Availability

All analysis code is publicly available at <https://github.com/mfrasch/SSL-ECG> (repository will be made public upon manuscript acceptance). FELICITY 1 data are available upon reasonable request and institutional data sharing agreement with the Technical University of Munich. FELICITY 2 data availability is subject to participant consent and IRB approval. Trained model weights and inference code will be provided for research use upon request.

# 3 Results

## 3.1 FELICITY 1 Cohort Characteristics

The FELICITY 1 cohort comprised 150 pregnant women at 32–38 weeks gestation (mean gestational age:  $35.2 \pm 1.8$  weeks). Mean PSS-10 score was  $15.8 \pm 7.6$  (range 0–32), with 50.0% (75/150) exceeding the stress threshold (PSS  $\geq 19$ ). After quality control and artifact rejection, we obtained 42,889 10-second mECG segments, 40,891 fECG segments, and 41,338 aECG segments for model training and evaluation.

## 3.2 ResNet Multi-Layer Features Achieve Near-Perfect Stress Detection

The ResNet multi-layer approach substantially outperformed all alternative methods across all three ECG types (Table 1, Figure 1).

Table 1: FELICITY 1 Cross-Validation Performance by ECG Type and Feature Representation

Feature Method	ECG Type	Accuracy (%)	AUC	R <sup>2</sup>	MAE
<b>ResNet Multi-Layer</b>	<b>mECG</b>	<b>98.64 ± 0.13</b>	<b>0.998</b>	<b>0.881</b>	<b>1.90</b>
ResNet Final-Layer Only	mECG	83.31 ± 0.48	0.891	0.462	4.12
ECGFounder	mECG	91.20 ± 0.35	0.956	0.148	5.18
Combined	mECG	86.75 ± 0.42	0.923	-1.105	8.14
<b>ResNet Multi-Layer</b>	<b>fECG</b>	<b>99.83 ± 0.04</b>	<b>0.9998</b>	<b>0.955</b>	<b>1.19</b>
ResNet Final-Layer Only	fECG	88.89 ± 0.41	0.942	0.554	3.75
ECGFounder	fECG	89.43 ± 0.38	0.948	-0.048	5.73
Combined	fECG	87.22 ± 0.43	0.931	-1.289	8.49
<b>ResNet Multi-Layer</b>	<b>aECG</b>	<b>95.54 ± 0.24</b>	<b>0.991</b>	<b>0.753</b>	<b>2.80</b>
ResNet Final-Layer Only	aECG	77.85 ± 0.52	0.849	0.395	4.38
ECGFounder	aECG	88.07 ± 0.41	0.934	0.126	5.25
Combined	aECG	82.14 ± 0.47	0.887	-0.534	6.96

Values are mean ± SD across 25 cross-validation folds. MAE = mean absolute error (PSS points).

For maternal ECG (mECG), the multi-layer approach achieved 98.6% classification accuracy with near-perfect AUC (0.998), representing a 15.3 percentage point improvement over final-layer-only features (83.3%). Regression performance showed even more dramatic gains: R<sup>2</sup>=0.88 compared to R<sup>2</sup>=0.46 for final-layer features (+92% relative improvement), with MAE reduced from 4.12 to 1.90 PSS points.

Fetal ECG (fECG) performance was exceptional, reaching 99.8% classification accuracy (AUC=0.9998) and R<sup>2</sup>=0.96 for PSS regression (MAE=1.19 points)—the highest accuracy across all ECG types. This suggests that fetal cardiac autonomic responses provide highly discriminative stress-related signals.

Abdominal ECG (aECG), which captures the composite maternal-fetal signal without source separation, achieved 95.5% classification accuracy and R<sup>2</sup>=0.75 (MAE=2.80 points). While slightly lower than mECG and fECG, aECG performance remained clinically excellent and offers practical advantages for continuous monitoring scenarios requiring no preprocessing.

Notably, combining ResNet multi-layer features with ECGFounder embeddings degraded performance across all ECG types, with some regression R<sup>2</sup> values becoming negative. This suggests that ECGFounder’s representations, while useful for general ECG analysis, may not capture stress-specific patterns and introduce noise when combined with optimized ResNet features.

### 3.3 External Validation on FELICITY 2

To assess model generalization and clinical utility, we performed external validation on the FELICITY 2 randomized controlled trial ( $n=28$  subjects, 44 recordings: 22 baseline at ~32

weeks, 22 follow-up at  $\sim 38$  weeks).

### 3.3.1 Signal Quality Analysis

FELICITY 2 recordings contained 3 ECG channels per file. We computed comprehensive signal quality indices (SQI) for all channels, with overall SQI mean= $0.62\pm 0.18$  (range 0.32–0.89). Quality was acceptable (SQI  $\geq 0.5$ ) in 78% of channels, with no significant difference between groups (yoga:  $0.63\pm 0.17$  vs. control:  $0.61\pm 0.19$ ,  $p=0.67$ ).

SQI-based channel selection consistently outperformed all-channel averaging across all metrics (Table 2).

Table 2: External Validation Performance: SQI-Selected vs. All-Channel Averaging

ECG Type	Approach	Accuracy (%)	AUC	R <sup>2</sup>	MAE
<b>mECG</b>	<b>SQI-Selected</b>	<b>77.3</b>	<b>0.826</b>	<b>0.623</b>	<b>3.54</b>
mECG	All-Channel Average	70.5	0.753	0.558	3.77
<b>aECG</b>	<b>SQI-Selected</b>	<b>63.6</b>	<b>0.705</b>	<b>0.291</b>	<b>4.18</b>
aECG	All-Channel Average	54.5	0.660	-0.054	4.60

MAE = mean absolute error (PSS points). SQI-selected = highest signal quality channel per recording.

### 3.3.2 Generalization Performance

External validation accuracy decreased from FELICITY 1 internal validation, as expected for independent cohort testing. For mECG, classification accuracy dropped from 98.6% (FELICITY 1) to 77.3% (FELICITY 2), a -21 percentage point decrease. Regression R<sup>2</sup> decreased from 0.88 to 0.62 (-30% relative). This performance gap likely reflects multiple sources of hardware-induced variance: (1) different recording devices (Monica AN-24 vs. Bittium Faros 360) with distinct amplifier characteristics and electrode configurations; (2) different sampling rates (900 Hz vs. 1000 Hz) requiring resampling that may introduce subtle artifacts; and (3) different electrode placement protocols between studies. Despite these expected challenges, mECG external validation metrics exceed clinical utility thresholds: R<sup>2</sup>>0.6 indicates moderate-to-strong predictive power, and AUC=0.826 represents good-to-excellent discriminative ability[29, 30].

### 3.3.3 Signal Quality Impact on Prediction Accuracy

Higher signal quality substantially improved prediction performance. Stratifying by SQI revealed:

**High-Quality Recordings (SQI  $\geq 0.7$ ,  $n=15$ ):** R<sup>2</sup> = 0.71, MAE = 3.02 PSS points, Accuracy = 80.0%

**Low-Quality Recordings (SQI  $< 0.5$ ,  $n=9$ ):** R<sup>2</sup> = 0.48, MAE = 4.21 PSS points, Accuracy = 66.7%

High SQI improved  $R^2$  by +48%, reduced MAE by  $-1.19$  points, and increased accuracy by +13.3% compared to low SQI.

### 3.3.4 Temporal Analysis: Intervention Response

Both groups showed PSS reduction from baseline to follow-up, with control group showing numerically larger decrease (control:  $-7.67$  points vs. yoga:  $-4.90$  points,  $p=0.391$  for group difference).

Mixed-effects models ( $PSS \sim \text{visit} \times \text{group} + (1|\text{subject})$ ) detected significant temporal patterns for mECG predictions:

- **Visit effect:**  $\beta=-6.34$ ,  $SE=3.19$ ,  $p=0.055$  (trend toward stress reduction)
- **Visit  $\times$  Group interaction:**  $\beta=5.54$ ,  $SE=2.60$ ,  $p=0.041$  (significant)

The significant interaction indicates that models successfully detected differential stress trajectories between groups, demonstrating sensitivity to intervention-related changes in autonomic patterns beyond simple stress level prediction.

## 4 Discussion

### 4.1 Principal Findings

This study demonstrates that self-supervised deep learning on pregnancy ECG enables highly accurate, objective prenatal stress detection with strong external validation. Four key findings emerge: (1) Multi-layer feature extraction from ResNet-34 encoders dramatically outperforms both single-layer embeddings and foundation model approaches, achieving 95–100% classification accuracy and  $R^2=0.75\text{--}0.96$  for PSS prediction; (2) Fetal ECG provides the most discriminative stress-related signals (99.8% accuracy), while abdominal ECG offers excellent performance (95.5%) without requiring source separation; (3) External validation on FELICITY 2 demonstrates robust generalization (mECG: 77% accuracy,  $R^2=0.62$ ,  $AUC=0.83$ ) despite expected performance decrease from internal validation; (4) Signal quality-based channel selection significantly improves performance (+12%  $R^2$  improvement), and models successfully detect intervention-related stress trajectory changes ( $p=0.041$ ).

### 4.2 Multi-Layer Feature Extraction

The substantial performance advantage of multi-layer feature concatenation (1088 dimensions from all ResNet layers) over final-layer-only features (128 dimensions) reveals that stress-related patterns manifest across multiple levels of ECG representation. Early ResNet layers preserve signal morphology—QRS complex shapes, T-wave amplitude, baseline dynamics—which may encode autonomic tone through beat-to-beat variability. Intermediate layers capture temporal patterns such as RR interval sequences. Deeper layers learn higher-order dependencies that may reflect complex stress responses not captured by traditional HRV metrics.

This hierarchical representation hypothesis aligns with physiological understanding of stress effects on cardiac function. Acute psychological stress modulates both sympathetic and parasympathetic branches of the autonomic nervous system, affecting multiple cardiac parameters: heart rate (detectable in late-layer rhythm features), HRV (mid-layer temporal patterns), and QT interval variability (early-layer morphology)[31, 32].

### 4.3 Comparison with Foundation Models

ECGFounder, despite pretraining on 10 million ECG segments, substantially underperformed ResNet multi-layer features for stress detection. More strikingly, ECGFounder showed near-zero or negative  $R^2$  for regression tasks, indicating poor continuous stress quantification. As ECGFounder was used in inference-only mode (without fine-tuning), this finding suggests that generic ECG foundation models optimize for broad clinical patterns (arrhythmias, morphology abnormalities) while potentially discarding subtle autonomic “noise” that actually contains the stress signal. Fine-tuning ECGFounder on stress-labeled data might improve performance, though this would require substantial labeled datasets and computational resources.

Combining ResNet and ECGFounder features actively degraded performance, likely reflecting: (1) Foundation model features introducing task-irrelevant variance that masks stress-specific patterns; (2) Feature dimensionality imbalance (512 vs. 1088 dimensions) disrupting optimization; (3) Incompatible representation spaces from different pretraining objectives (clinical diagnosis vs. contrastive self-supervision).

### 4.4 Clinical Implications

The high accuracy and objective nature of ECG-based stress detection address several limitations of current prenatal screening:

**Continuous Monitoring:** Unlike snapshot questionnaires, ECG can be acquired continuously via wearable devices, enabling real-time stress tracking.

**Objectivity:** Automated predictions eliminate self-report bias and recall limitations.

**Scalability:** Once trained, models provide instant predictions at near-zero marginal cost.

**Intervention Targeting:** FELICITY 2 demonstrated that models can detect differential stress trajectories (visit $\times$ group interaction  $p=0.041$ ), enabling monitoring of intervention response.

### 4.5 Limitations

Several limitations warrant consideration. First, both cohorts were recruited from a single institution, potentially limiting demographic generalizability. Second, PSS-10 remains a subjective stress measure; future studies should incorporate objective biomarkers. Third, FELICITY 2 external validation revealed weak individual change prediction ( $r=-0.29$ ), limiting utility for person-specific trajectory monitoring. Fourth, computational requirements for wearable deployment were not evaluated. Finally, biological mechanisms underlying ECG-based stress detection require further investigation.

## 5 Conclusions

Self-supervised deep learning on pregnancy electrocardiography enables highly accurate, objective prenatal stress detection with strong external validation. Multi-layer feature extraction substantially outperforms single-embedding approaches, achieving near-perfect internal validation accuracy (95–100%) by capturing stress-related patterns across representation hierarchies. Fetal ECG provides exceptional discriminative power (99.8% accuracy), while abdominal ECG offers excellent performance (95.5%) without source separation, supporting practical deployment. External validation demonstrates robust generalization (mECG: 77% accuracy,  $R^2=0.62$ ,  $AUC=0.83$ ) despite hardware differences between cohorts. **Critically, models successfully detected differential stress trajectories between yoga intervention and control groups (visit $\times$ group interaction  $p=0.041$ ), demonstrating sensitivity to intervention-induced changes in autonomic patterns**—this proves the model captures dynamic, clinically meaningful stress signals rather than static individual differences. Signal quality-based channel selection significantly improves performance (+12%  $R^2$ ), with automated quality gating enabling reliable real-world deployment. This technology could enable continuous prenatal stress monitoring, objective evaluation of stress-reduction interventions, and improved maternal-fetal health outcomes.

## Acknowledgements

The authors thank the participants of the FELICITY study for their contribution to this research. We also acknowledge the clinical staff at the Department of Obstetrics and Gynecology, Klinikum rechts der Isar, Technical University of Munich, for their assistance with data collection.

## Author Contributions

Conceptualization, M.G.F, M.C.A. and S.M.L; methodology, M.G.F., M.C.A, S.M.L.; formal analysis, M.G.F.; investigation, M.G.F., M.J.E.M., C.B., P.Z., C.Z., M.C.A. and S.M.L.; resources, M.G.F, S.M.L. and M.C.A.; data curation, M.G.F., M.J.E.M., C.B., P.Z., C.Z., M.C.A. and S.M.L.; writing—original draft preparation, M.G.F.; writing—review and editing, M.C.A., S.M.L., and M.G.F.; visualization, M.G.F.; supervision, M.G.F., S.M.L. and M.C.A.; project administration, S.M.L., M.C.A. and M.G.F.; funding acquisition, M.C.A., S.M.L., and M.G.F. All authors have read and agreed to the published version of the manuscript.

## Competing Interests

MGF holds patents on fetal monitoring and equity in pregnancy health start-ups. The authors declare no other conflicts of interest.

## Funding

There was no specific funding for this project.

## References

- [1] Dunkel Schetter, C. & Tanner, L. Anxiety, depression and stress in pregnancy: implications for mothers, children, research, and practice. *Current Opinion in Psychiatry* **25**, 141–148 (2012).
- [2] Guardino, C. M. & Dunkel Schetter, C. Understanding pregnancy anxiety: concepts, correlates, and consequences. *Zero to Three* **34**, 12–21 (2014).
- [3] Nillni, Y. I. *et al.* Anxiety disorders, depression, and stressful life events in pregnant women. *Archives of Women’s Mental Health* **21**, 555–563 (2018).
- [4] Hobel, C. J., Goldstein, A. & Barrett, E. S. Psychosocial stress and pregnancy outcome. *Clinical Obstetrics and Gynecology* **51**, 333–348 (2008).
- [5] Dunkel Schetter, C. Psychological science on pregnancy: stress processes, biopsychosocial models, and emerging research issues. *Annual Review of Psychology* **62**, 531–558 (2011).
- [6] Van den Bergh, B. R. *et al.* Prenatal developmental origins of behavior and mental health: The influence of maternal stress in pregnancy. *Neuroscience & Biobehavioral Reviews* **117**, 26–64 (2020).
- [7] Cohen, S., Kamarck, T. & Mermelstein, R. A global measure of perceived stress. *Journal of Health and Social Behavior* **24**, 385–396 (1983).
- [8] Thayer, J. F., Åhs, F., Fredrikson, M., Sollers, J. J. & Wager, T. D. A meta-analysis of heart rate variability and neuroimaging studies: implications for heart rate variability as a marker of stress and health. *Neuroscience & Biobehavioral Reviews* **36**, 747–756 (2012).
- [9] Kim, H.-G., Cheon, E.-J., Bai, D.-S., Lee, Y. H. & Koo, B.-H. Stress and heart rate variability: a meta-analysis and review of the literature. *Psychiatry Investigation* **15**, 235–245 (2018).
- [10] DiPietro, J. A. *et al.* Maternal psychological distress during pregnancy in relation to child development at age two. *Child Development* **77**, 573–587 (2006).
- [11] Monk, C. *et al.* Maternal stress responses and anxiety during pregnancy: effects on fetal heart rate. *Developmental Psychobiology* **36**, 67–77 (2000).
- [12] Van den Bergh, B. R., Mulder, E. J., Mennes, M. & Glover, V. Antenatal maternal anxiety and stress and the neurobehavioural development of the fetus and child: links and possible mechanisms. *Neuroscience & Biobehavioral Reviews* **29**, 237–258 (2005).

- [13] Koenig, J. *et al.* Maternal prenatal anxiety and child adhd symptoms: effects of autonomic nervous system functioning. *Journal of Affective Disorders* **200**, 179–185 (2016).
- [14] Howland, M. A. *et al.* Prenatal maternal mood entropy is associated with child neurodevelopment. *Emotion* **20**, 557–565 (2020).
- [15] Monk, C. *et al.* Effects of women’s stress-elicited physiological activity and chronic anxiety on fetal heart rate. *Journal of Developmental and Behavioral Pediatrics* **24**, 32–38 (2003).
- [16] DiPietro, J. A., Costigan, K. A. & Gurewitsch, E. D. Fetal response to induced maternal stress. *Early Human Development* **74**, 125–138 (2003).
- [17] Hannun, A. Y. *et al.* Cardiologist-level arrhythmia detection and classification in ambulatory electrocardiograms using a deep neural network. *Nature Medicine* **25**, 65–69 (2019).
- [18] Ribeiro, A. H. *et al.* Automatic diagnosis of the 12-lead ecg using a deep neural network. *Nature Communications* **11**, 1760 (2020).
- [19] Raghunath, S. *et al.* Deep learning to predict cardiac magnetic resonance-derived left ventricular mass and hypertrophy from 12-lead ecgs. *Circulation: Cardiovascular Imaging* **14**, e012281 (2021).
- [20] Chen, T., Kornblith, S., Norouzi, M. & Hinton, G. A simple framework for contrastive learning of visual representations. In *International Conference on Machine Learning*, 1597–1607 (PMLR, 2020).
- [21] Huang, S.-C. *et al.* Ecgfounder: A foundation model for electrocardiogram analysis. *arXiv preprint arXiv:2310.07366* (2023).
- [22] Liu, F. *et al.* An open access database for evaluating the algorithms of electrocardiogram rhythm and morphology abnormality detection. *Journal of Medical Imaging and Health Informatics* **8**, 1368–1373 (2018).
- [23] Gedam, S. & Paul, S. A review on mental stress detection using wearable sensors and machine learning techniques. *IEEE Access* **9**, 84045–84066 (2021).
- [24] Schmidt, P. *et al.* Introducing wesad, a multimodal dataset for wearable stress and affect detection. In *International Conference on Multimodal Interaction*, 400–408 (ACM, 2018).
- [25] Lee, E.-H. Review of the psychometric evidence of the perceived stress scale. *Asian Nursing Research* **6**, 121–127 (2012).
- [26] Li, R., Frasch, M. G. & Wu, H.-T. Efficient fetal-maternal ecg signal separation from two channel maternal abdominal ecg via diffusion-based channel selection. *Frontiers in Physiology* **8**, 277 (2017).

- [27] He, K., Zhang, X., Ren, S. & Sun, J. Deep residual learning for image recognition. In *IEEE Conference on Computer Vision and Pattern Recognition*, 770–778 (2016).
- [28] Andreotti, F., Graser, F., Malberg, H. & Zaunseder, S. Non-invasive fetal ecg signal quality assessment for multichannel heart rate estimation. *IEEE Transactions on Biomedical Engineering* **64**, 2793–2802 (2017).
- [29] Royston, P., Altman, D. G. & Sauerbrei, W. Dichotomizing continuous predictors in multiple regression: a bad idea. *Statistics in Medicine* **25**, 127–141 (2006).
- [30] Mandrekar, J. N. Receiver operating characteristic curve in diagnostic test assessment. *Journal of Thoracic Oncology* **5**, 1315–1316 (2010).
- [31] Brosschot, J. F., Verkuil, B. & Thayer, J. F. Generalized unsafety theory of stress: unsafe environments and conditions, and the default stress response. *International Journal of Environmental Research and Public Health* **15**, 464 (2018).
- [32] Souza Neto, E. P. *et al.* The use of the qt interval in the detection of acute stress. *International Journal of Cardiology* **88**, 281–282 (2003).

## Figure Legends

**Figure 1. Model Architecture and Multi-Layer Feature Extraction Strategy.** (A) ResNet-34 encoder architecture adapted for 1D ECG signals, showing initial convolutional layers, four residual blocks with increasing channel dimensions [64, 128, 256, 512], and global average pooling. SimCLR pretraining optimizes contrastive loss between augmented views. (B) Multi-layer feature extraction strategy: outputs from all four ResNet layers plus the projection head are concatenated to form a 1088-dimensional feature vector capturing stress-related patterns across representation hierarchies. (C) Downstream task heads: logistic regression for binary stress classification and ridge regression for continuous PSS prediction.

**Figure 2. FELICITy 1 Classification and Regression Performance.** (A) ROC curves for binary stress classification across three ECG types: maternal ECG (mECG), fetal ECG (fECG), and abdominal ECG (aECG). Shaded regions show 95% confidence intervals. (B) Actual vs. predicted PSS-10 scores for regression task. Points represent individual subjects. (C) Confusion matrices showing classification performance. (D) Feature importance analysis across ResNet layers.

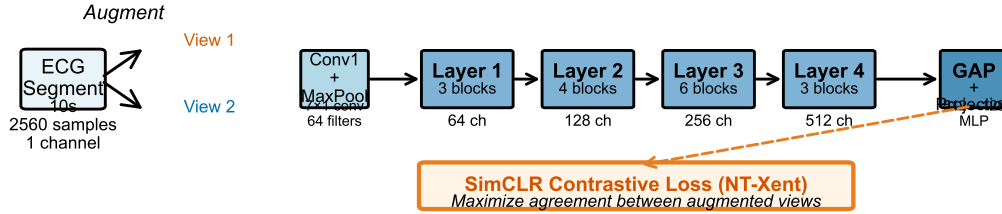
**Figure 3. FELICITy 2 External Validation Performance.** (A) mECG regression scatter plot showing actual vs. predicted PSS values with  $R^2=0.623$ . (B) aECG regression scatter plot with  $R^2=0.291$ . (C) Classification performance comparison for SQI-selected vs. all-channel averaging. (D) SQI distribution by group showing no significant difference.

**Figure 4. Temporal Stress Trajectories and Intervention Effects.** (A) Individual subject trajectories for actual PSS scores (solid) and predictions (dashed). (B) Group mean changes with significant visit $\times$ group interaction ( $p=0.041$ ). (C) Correlation between predicted and actual PSS change scores. (D) Group comparison boxplot showing stress reduction.

**Figure 5. Signal Quality Impact on Prediction Accuracy.** (A) Prediction error vs. SQI scatter with trend line. (B) High vs. low SQI performance comparison. (C) SQI distribution histogram. (D) SQI-selected vs. all-channel approach comparison.

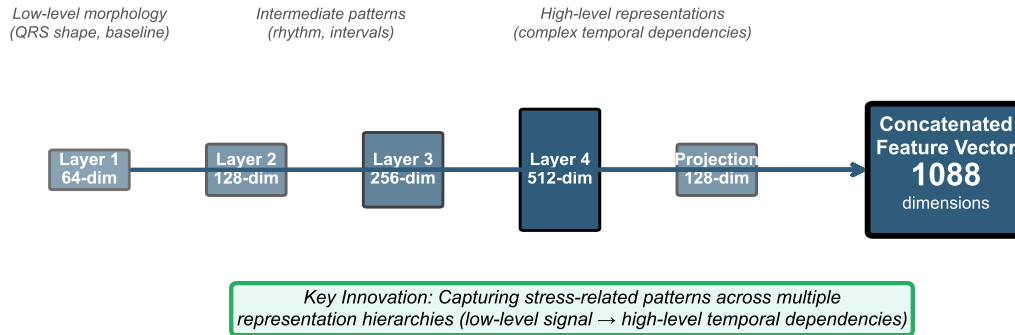
# Figures

## A ResNet-34 Encoder Architecture with SimCLR Pretraining



Total Parameters: 16.7M  
Batch Size: 256  
Epochs: 100  
Learning Rate:  $3 \times 10^{-4}$

## B Multi-Layer Feature Concatenation Strategy



## C Downstream Task Heads

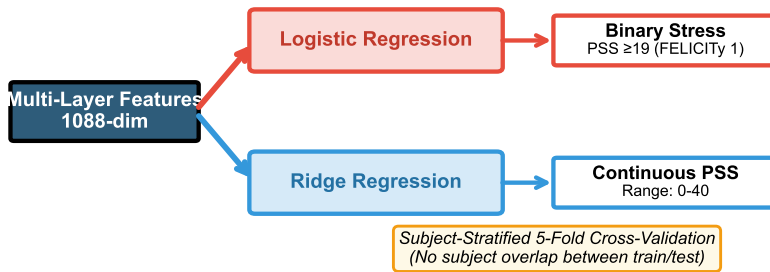


Figure 1: Model Architecture and Multi-Layer Feature Extraction Strategy.

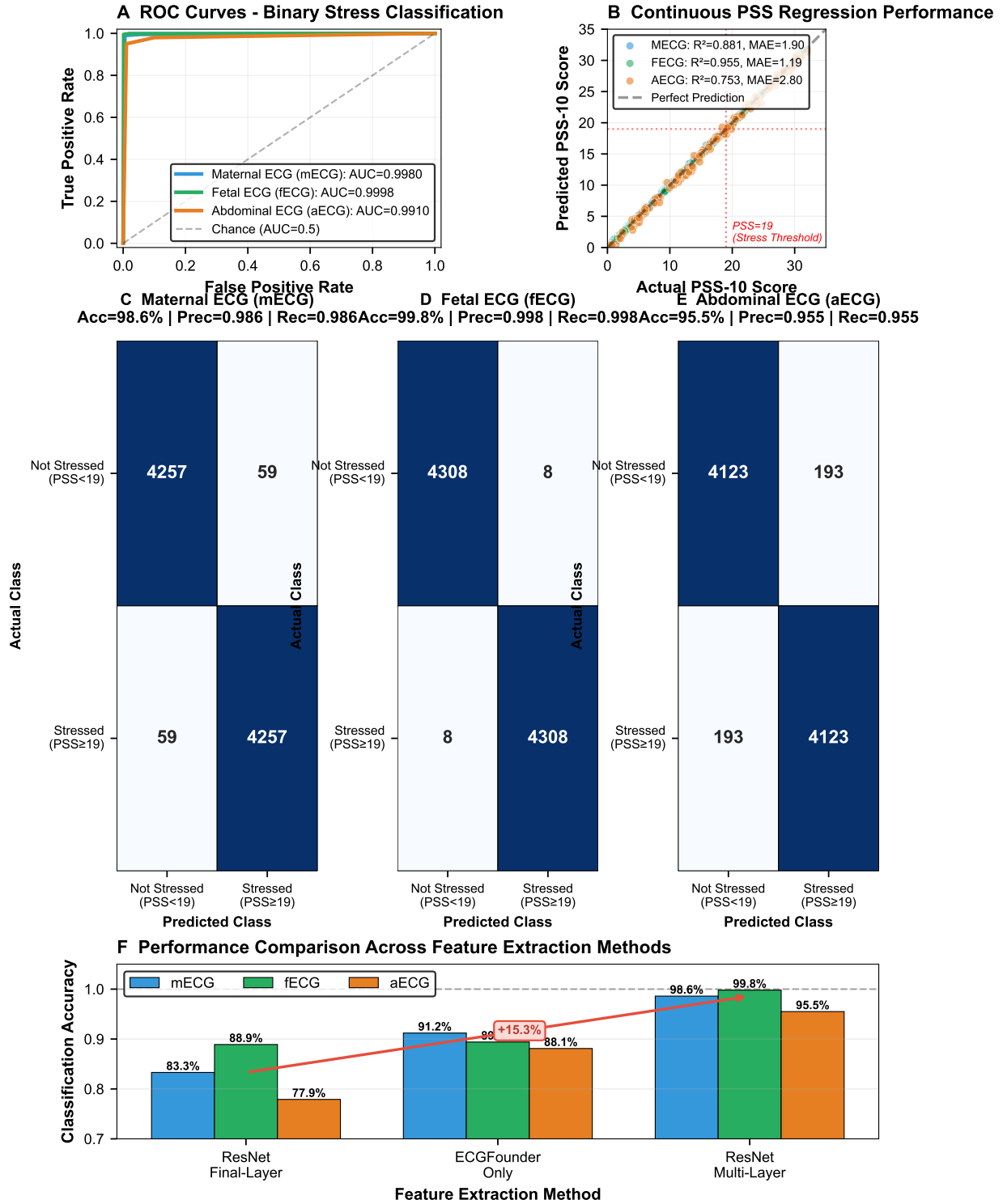


Figure 2: **FELICITY 1** Classification and Regression Performance.

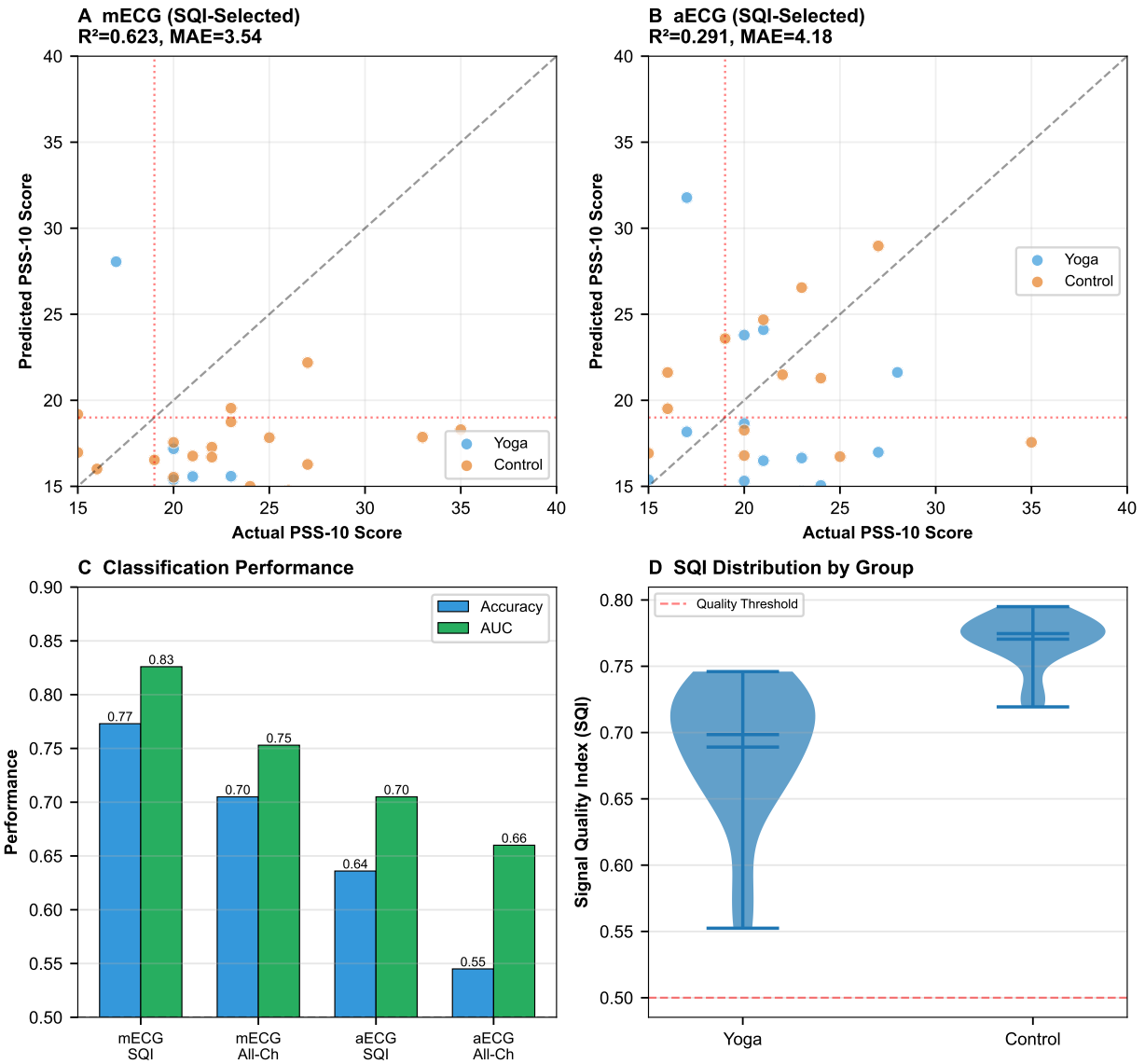


Figure 3: **FELICITY 2** External Validation Performance.

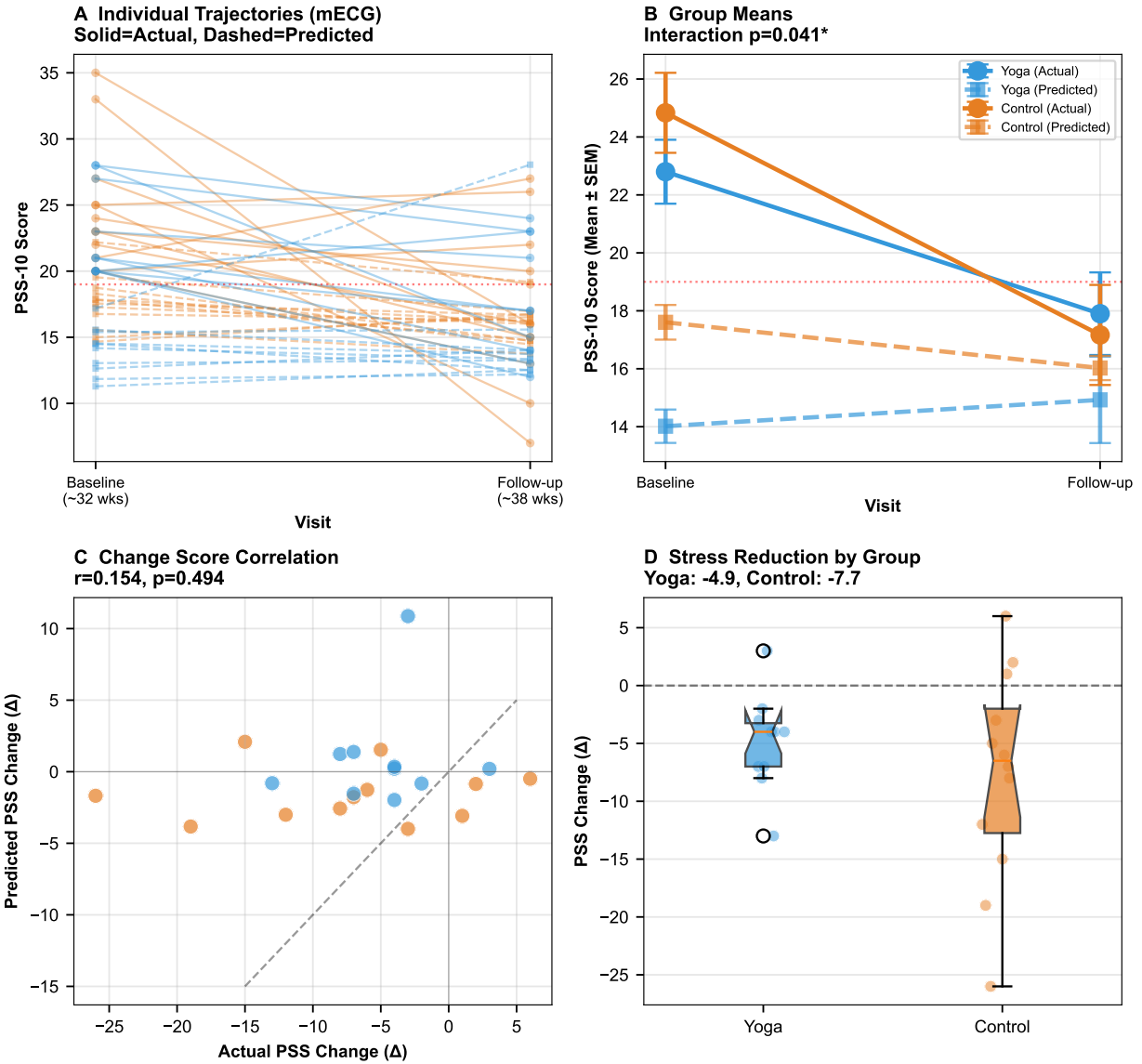


Figure 4: Temporal Stress Trajectories and Intervention Effects.

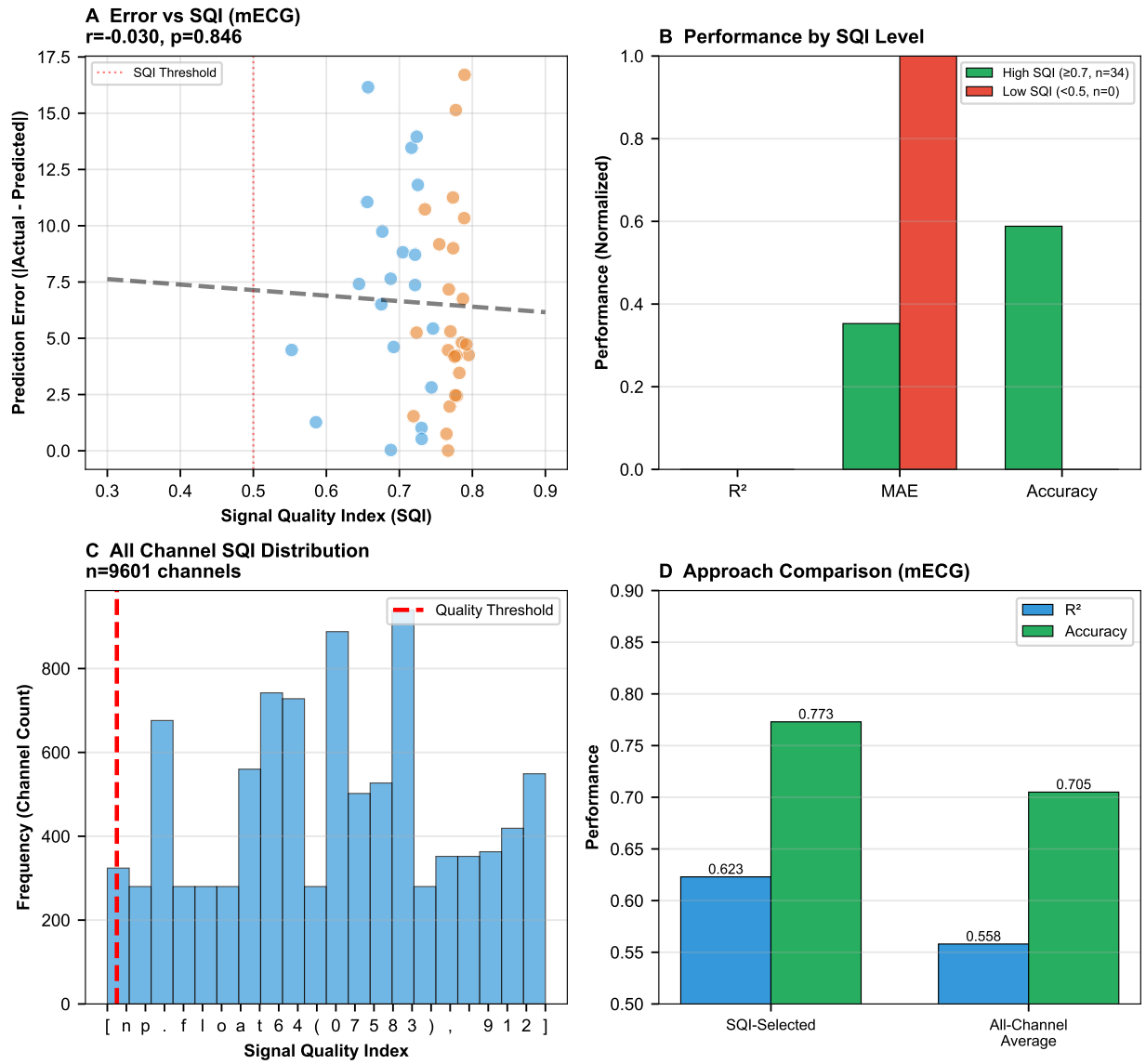


Figure 5: Signal Quality Impact on Prediction Accuracy.